NEOPLASIA
www.neoplasia.com

Volume 19 Number 8 August 2017 pp. 637–648 637

Combined Inhibition of CDK4/6 and PI3K/AKT/mTOR Pathways Induces a Synergistic Anti-Tumor Effect in Malignant Pleural Mesothelioma Cells[1]

Mara A. Bonelli*, Graziana Digiacomo*, Claudia Fumarola*, Roberta Alfieri*, Federico Quaini[a], Angela Falco*, Denise Madeddu*, Silvia La Monica*, Daniele Cretella*, Andrea Ravelli*, Paola Ulivi[†], Michela Tebaldi[†], Daniele Calistri[†], Angelo Delmonte[‡], Luca Ampollini*, Paolo Carbognani*, Marcello Tiseo[§], Andrea Cavazzoni*,[2] and Pier Giorgio Petronini*,[2]

*Department of Medicine and Surgery, University of Parma, Via Gramsci 14, 43126 Parma, Italy; [†]Biosciences Laboratory, IRST-IRCCS, Meldola, Italy; [‡]Department of Medical Oncology, IRST-IRCCS, Meldola, Italy; [§]Division of Medical Oncology, University Hospital of Parma, Parma, Italy

Abstract

Malignant pleural mesothelioma (MPM) is a progressive malignancy associated to the exposure of asbestos fibers. The most frequently inactivated tumor suppressor gene in MPM is *CDKN2A/ARF*, encoding for the cell cycle inhibitors $p16^{INK4a}$ and $p14^{ARF}$, deleted in about 70% of MPM cases. Considering the high frequency of alterations of this gene, we tested in MPM cells the efficacy of palbociclib (PD-0332991), a highly selective inhibitor of cyclin-dependent kinase (CDK) 4/6. The analyses were performed on a panel of MPM cell lines and on two primary culture cells from pleural effusion of patients with MPM. All the MPM cell lines, as well as the primary cultures, were sensitive to palbociclib with a significant blockade in G0/G1 phase of the cell cycle and with the acquisition of a senescent phenotype. Palbociclib reduced the phosphorylation levels of CDK6 and Rb, the expression of myc with a concomitant increased phosphorylation of AKT. Based on these results, we tested the efficacy of the combination of palbociclib with the PI3K inhibitors NVP-BEZ235 or NVP-BYL719. After palbociclib treatment, the sequential association with PI3K inhibitors synergistically hampered cell proliferation and strongly increased the percentage of senescent cells. In addition, AKT activation was repressed while p53 and p21 were up-regulated. Interestingly, two cycles of sequential drug administration produced irreversible growth arrest and senescent phenotype that were maintained even after drug withdrawal. These findings suggest that the sequential association of palbociclib with PI3K inhibitors may represent a valuable therapeutic option for the treatment of MPM.

Neoplasia (2017) 19, 637–648

Abbreviations: MPM, Malignant Pleural Mesothelioma; BAP1, BRCA1 Associated Protein 1; CDK, Cyclin-dependent kinase; RB, Retinoblastoma Protein; SA-β-GAL, Senescence Associated β-Galactosidase

Address all correspondence to: Mara A. Bonelli or Claudia Fumarola.
E-mail: mara.bonelli@unipr.it

[1] FundingThis work was supported by:
Associazione Augusto per la Vita (Novellara, RE), grant to P.G. Petronini and to A. Delmonte; Associazione Noi per Loro onlus (Parma), fellowship to Graziana Digiacomo; CHIESI Farmaceutici S.p.A. (Parma), grant to P.G. Petronini; Transfer Oil S.p.A. (Colorno, PR), grant to P.G. Petronini; Famiglia Gigetto Furlotti (Parma); Fondazione Italiana Biologi-Ordine Nazionale dei Biologi (Roma)

[2] Co-last authors

Received 7 April 2017; Revised 10 May 2017; Accepted 15 May 2017

1476-5586
http://dx.doi.org/10.1016/j.neo.2017.05.003

Introduction

Malignant pleural mesothelioma (MPM) is a progressive, poor prognosis malignancy of the pleura associated to the exposure to asbestos fibers. Due to the long latency period of this disease, the incidence of mesothelioma is expected to peak around the next 5–10 years [1]. Systemic chemotherapy remains one of the main treatments to prolong survival, nevertheless, the mean overall survival of MPM patients is limited to about 12 months and the median progression free survival is less than 6 months due to the intrinsic chemo-resistance of the disease. Based on the increasing incidence and the poor prognosis of MPM, novel therapeutic strategies are under investigation [2].

Several genetic alterations have been recently identified in MPM pathogenesis. However, MPM is being characterized mostly by the loss of tumor suppressor genes, rather than activation of oncogenes and an oncogenic driver is still lacking. The most frequently inactivated tumor suppressor genes in MPM are *CDKN2A/ARF*, deleted in about 70% of MPM cases, neurofibromin 2 (*NF2*), encoding for merlin and inactivated in 40–50% of MPM cases, and BRCA1 associated protein 1 (*BAP1*), gene associated to familial MPMs [3,4].

The *CDKN2A/ARF* tumor suppressor gene encodes for two cell cycle regulatory proteins: cyclin dependent kinase inhibitor 2A ($p16^{INK4a}$) and alternate reading frame ($p14^{ARF}$). *cdkn2a* and *arf* are regulated by separate promoters, differ in the first exon (exon 1alpha and 1beta respectively), share exons 2 and 3, and are translated from alternative reading frames [5]. $p16^{INK4a}$ inhibits the formation of the complex cyclin D1/CDK4/6 by binding to CDK4/6 and thereby maintaining retinoblastoma protein (Rb) in its hypophosphorylated active form, with consequent G1 cell cycle arrest. $p14^{ARF}$ binds to MDM2 and inhibits MDM2-induced degradation of p53, enhancing p53-dependent transactivation, cell cycle arrest and/or apoptosis. Deletion of the *CDKN2A/ARF* locus facilitates cell cycle progression, escape from apoptosis and immortalization.

Palbociclib (PD-0332991) is an oral-available, highly selective inhibitor of CDK4/6 kinase activity that inhibits Rb phosphorylation and therefore prevents cellular DNA synthesis by inhibiting progression of the cell cycle from G1 to S phase. Currently, palbociclib is approved by the US FDA (Food and Drug Administration), for the treatment of estrogen positive metastatic breast cancer in association with letrozole. Palbociclib usually presents tolerable toxicity with mild neutropenia and thrombocytopenia as main adverse events. Considering the high frequency of deletion of *CDKN2A/ARF* in MPM, we investigated the effect of palbocilib on a panel of MPM cell lines and on cells obtained from pleural effusion of MPM patients.

One feature related to palbociclib treatment is the increased activation of the AKT/mTOR pathway, due to the increased phosphorylation of AKT, as recently reported by Zhang and coworkers [6] and confirmed in mesothelioma cells in our study. By inhibiting the TSC1–TSC2 complex, AKT activates the serine–threonine kinase mTOR, which exists in two distinct complexes, mTORC1 and mTORC2, upon binding with different regulatory proteins [7]. The PI3K/AKT/mTOR pathway plays a critical role in the control of cell growth, proliferation, metabolism, and migration, and is frequently deregulated in cancer cells, thus representing an attractive candidate for targeted cancer agents.

Thus, the present work was addressed to evaluate the antitumor potential of combining palbociclib with inhibitors of the PI3K/AKT/mTOR pathway in MPM cells. In particular, we tested the effect of the combination with NVP-BEZ235, a reversible competitive inhibitor of the ATP-binding site of both class I PI3K and mTOR [8], and NVP-BYL719, a specific inhibitor of the p110α subunit of class I PI3K [9].

Our findings demonstrated that, in comparison with individual treatments, the sequential association of palbociclib and PI3K/mTOR inhibitors enhanced the inhibition of cell proliferation (both in 2D and 3D cultures) and the induction of cell senescence; moreover, these effects were maintained after drug removal, suggesting a new therapeutic strategy to challenge the aggressive behavior of MPM.

Material and Methods

Cell Lines and Drugs

Human MPM cell lines MSTO-211H (biphasic histotype), H2452, H28 (both of epithelioid histotype), H2052 (sarcomatoid histotype) and MDA-MB-468 breast cancer cells were obtained from ATCC (Manassas, VA), cultured as recommended and maintained at 37 °C in a humidified atmosphere containing 5% CO_2.

ZS-LP e MG-LP primary cell lines were obtained from two patients (both male, 66 years for ZS-LP, 62 years for MG-LP) affected by mesothelioma biphasic histotype of stage T4 N0 for ZS-LP and T3 N0 for MG-LP, diagnosed at the Department of Pathology -University/Hospital of Parma. Patients were enrolled after informed consent to the employment of biologic samples for research purpose. The procedure was approved by the institutional review board for human studies (Ethical Committee) of the University-Hospital of Parma and in accord with principles listed in the Helsinki declaration. Pleural effusions were collected and transferred under sterile conditions. After centrifugation at 240 x g for 5 min at room temperature (RT), red blood cells were lysed and the pellet was suspended in fresh medium. ZS-LP e MG-LP cells were then cultured in RPMI supplemented with 2 mM glutamine, 10% FBS, non-essential amino acids (NEAA) and 100 U/ml penicillin, 100 µg/ml streptomycin. Cells were maintained at 37 °C in a humidified atmosphere containing 5% CO_2. Daily microscopic observation of the cultures showed the growth of a population of adherent cells whose MPM phenotype was assessed by the immunocytochemical analysis of Calretinin, HBME-1 and panCytokeratin.

Palbociclib (PD-0332991) was obtained from Selleckchem (Houston, TX); NVP-BEZ235 and NVP-BYL719 (hereafter, referred to as BEZ235 and BYL719) were provided by Novartis Institutes for BioMedical Research (Basel, Switzerland). Palbociclib was dissolved in bi-distilled sterile water, BEZ235 and BYL719 were prepared in DMSO and DMSO concentration never exceeded 0.1% (v/v); equal amounts of the solvent were added to control cells.

Western Blotting

Total cell lysates and Western blotting were performed as previously described [10].

Antibodies against p-Rb(Ser780), Rb, p-ERK1/2(Thr202/Tyr204), ERK1/2, p-AKT(Ser473), p-AKT(Thr308), p-AKT(Ser473), AKT, p-mTOR(Ser2448), mTOR, p-p70S6K(Thr389), p70S6K, $p21^{Waf1/Cip1}$, cyclin D1, CDK6, c-Myc, p-MDM2(Ser166) were from Cell Signaling Technology, Incorporated (Danvers, MA); anti-p53-(DO-1) and anti-p-CDK6(Tyr24) were from Santa Cruz

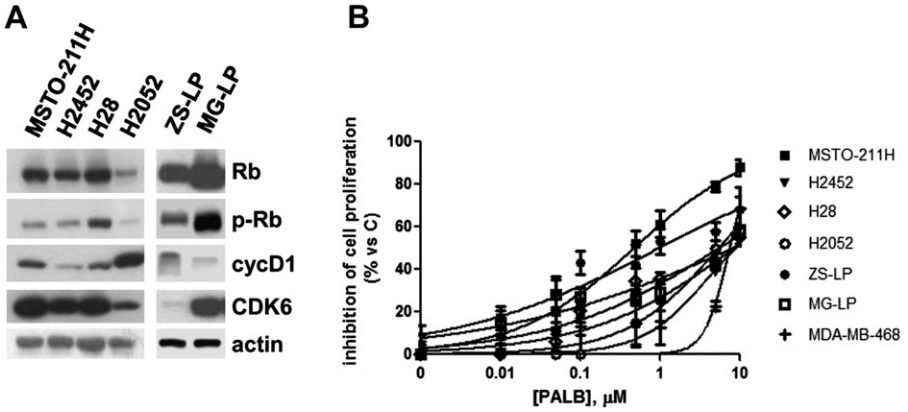

CELL LINE	EC50, μM
MSTO-211H	0.28 ± 0.14
H2452	0.7 ± 0.12
H28	0.33 ± 0.11
H2052	1.2 ± 0.1
ZS-LP	0.1 ± 0.02
MG-LP	0.3 ± 0.01
MDA-MB-468	5 ± 0.2

Figure 1. Palbolcilib sensitivity of MPM cells. (A) The expression level of proteins involved in the regulation of cell cycle was evaluated in MPM cell lines (MSTO-211H, H2452, H28, H2052) and in two primary cultures from pleural effusion (ZS-LP and MG-LP) by Western blotting. The experiment repeated twice yielded similar results. (B-C) After 24 h from seeding, the indicated cell lines were treated with increasing concentrations of palbociclib for 72 h. Cells proliferation was assessed by MTT assay and data are expressed as a percentage of inhibition versus control. EC_{50} values were calculated using GraphPad Prism 6.00 software. Experiments in B-C are the mean value ± SD of three independent measurements.

Biotechnology, Incorporated (Dallas, TX). Anti CDKN2A/p16^{INK4a} was from Abcam (Cambridge, UK). Anti-β-actin (clone B11V08) was from BioVision (Milpitas, CA). Horseradish peroxidase-conjugated secondary antibodies and chemiluminescence system were from Millipore (Millipore, MA). Reagents for electrophoresis and blotting analysis were from BIO-RAD Laboratories (Hercules, CA).

Analysis of Cell Proliferation and Cell Death

Cell viability was evaluated by cell counting, MTT assay and crystal violet assay as previously described [11]. Cell death was analyzed as described elsewhere [12]. The nature of interaction between palbociclib and PI3K inhibitors was calculated using the Bliss additivism model as previously described [13].

Analysis of Cell Cycle

Distribution of the cells in the cell cycle was determined as previously described [14].

Quantitative Real-Time PCR

Total RNA was isolated by RNeasy Mini Kit (Qiagen, Venlo, Netherlands) and the quantitative real-time polymerase chain reaction (PCR) was performed as previously described [15]. Primer for CDKN2A (QT00089964), HPRT1 (QT00059066) and PGK1 (QT00013776) were purchased from Qiagen.

Spheroid Generation and Growth

Spheroids from MSTO-211H were generated using LIPIDURE®-COAT PLATE A-U96 (NOF Corporation, Japan) according to manufacturer's instruction. Briefly, 200 cells were seeded and after 1–3 days the spheroids were formed and treated with drugs or vehicle for 96 hours. The effects of the drugs were evaluated in terms of volume changes as previously described [16].

β-Galactosidase Staining

The evaluation of Senescence Associated β-Galactosidase (SA-β-Gal) expression was performed using the Senescence β-Galactoside Staining kit (Cell Signaling Technology Inc.). Briefly, cells were seeded in 6-well plates (3 x 10^4 cells/well) in complete medium for 24 hours and then treated with drugs or vehicle. Finally, fixative solution was added for 15 minutes at room temperature. The plates were washed two times with PBS and then the β-Galactosidase staining solution was added. After overnight incubation at 37 °C without CO_2, the number of SA-β-Gal positive cells (blue stained) was evaluated by cell counting in five randomly chosen microscope fields (200× magnification).

Cell Line Molecular Characterization

Genomic DNA was extracted from the cell lines (ZS-LP and MG-LP) using QIAamp DNA mini kit (Qiagen). The extracted

Table 1. NGS Analyses of Primary Culture of MG-LP and ZS-LP Cells

Cell Line	Gene	Variant	Localization	Variant Effect	Protein Change	Annotation	Depth
ZS-LP	*PMS2*	c.2192_2196del	Exonic	deletion	p.L731 fs	rs63750695	1274
MG-LP	*BAP1*	c.758delA	Exonic	deletion	p.Q2563fs	-	363
ZS-LP MG-LP	*XPC*	c.C2815A	Exonic	missense	p.Q939K	rs2228001	402–253
ZS-LP MG-LP	*CHRNA3*	c.C645T	Exonic	synonymous	p.Y215Y	rs1051730	566–432

Sequencing runs produced a total of 11,683,490 reads, of which 99.92% mapped on the hg19 human reference genome, with a median coverage depth of 621.81× per sample on all target. The bases of the entire target with a coverage at least 200× was 89.65%.

660 and 580 variants were founded in MG-LP and ZS-LP cells respectively and, after adopting bioinformatic filters (exon and splicing variants, coverage variant >200× and a variant frequency of >10%, annotation into public databases – dbSNP, Clinical Variants, cosmic), 48 and 52 variants were selected into MG-LP and ZS-LP cells respectively.

In MG-LP we found 3 interesting variants, 1 deletion in *BAP1*, 1 missense in *XPC* and 1 in *CHRNA3*. Into ZS-LP line two variants in common with MG-LP line, *XPC* and *CHRNA3* variants, and one deletion into *PMS2* were found.

a

	G0-G1 %		S %		G2-M %	
	C	Palb	C	Palb	C	Palb
MSTO-211H	49 ± 3	78 ± 5	25 ± 3	11 ± 3	26 ± 1	11 ± 3
H2452	60 ± 2	74 ± 3	18 ± 4	14 ± 2	22 ± 3	12 ± 1
H28	62 ± 7	88 ± 3	16 ± 2	7 ± 1	22 ± 5	5 ± 1
H2052	79 ± 4	86 ± 3	12 ± 3	6 ± 1	9 ± 1	8 ± 1
ZS-LP	53 ± 5	83 ± 1	24 ± 6	6 ± 2	23 ± 4	11 ± 2
MG-LP	65 ± 3	75 ± 1	15 ± 3	9 ± 1	20 ± 2	16 ± 1
MDA-MB-468	41 ± 2	43 ± 4	36 ± 3	37 ± 5	23 ± 3	20 ± 5

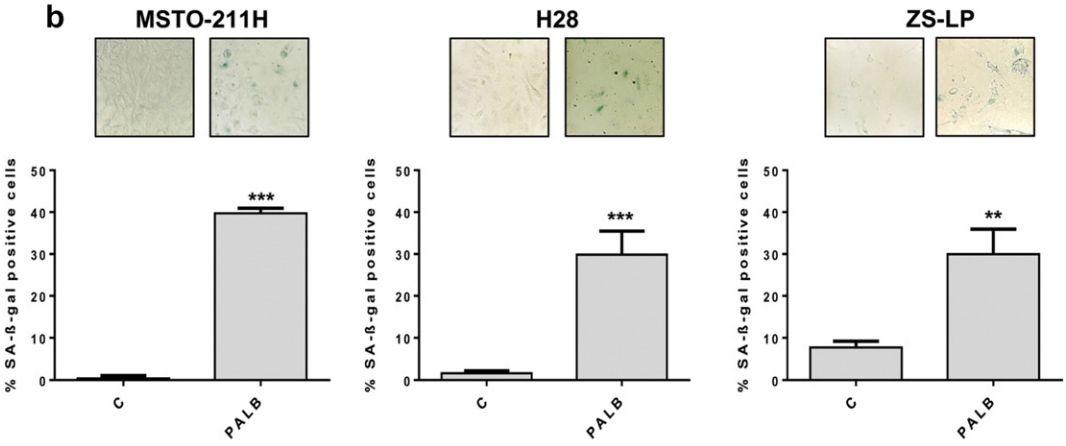

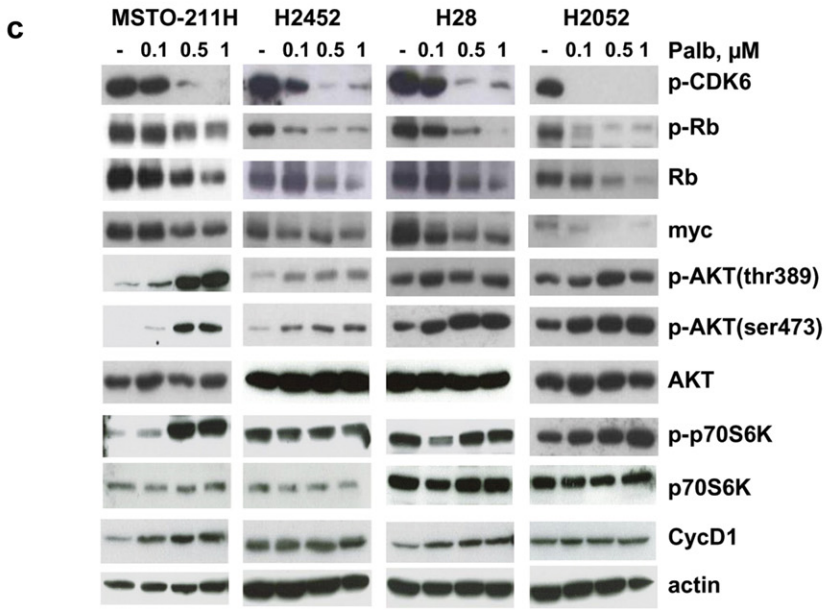

Figure 2. Palbociclib treatment induced cell cycle blockade and senescence. (A) Cells were maintained in the absence (C) or in the presence of palbociclib 0.5 μM (Palb). After 24 h the cells were stained with propidium iodide and cell-cycle-phase distribution was determined by flow cytometry. Data are expressed as a percentage of distribution in each cell-cycle phase. (B) MSTO-211H, H28 and ZS-LP cells were treated with palbociclib 0.5 μM for 72 h. The images are representative fields of cells stained with SA-β-Gal Staining kit. Histograms represent the percentage of senescent cells positive for SA-β-Gal expression and are means ±SD of data from three independent experiments (**$P < .01$, ***$P < .001$ versus C; student's t test). (C) MSTO-211H, H2452, H28 and H2052 cell lines were treated with increasing concentrations of palbociclib (0.1, 0.5 and 1 μM) for 24 h. The cells were lysed and the expression of the indicated proteins was evaluated by Western blot analysis. The experiment repeated twice yielded similar results. Experiments in A and B are the mean value ±SD of three independent measurements.

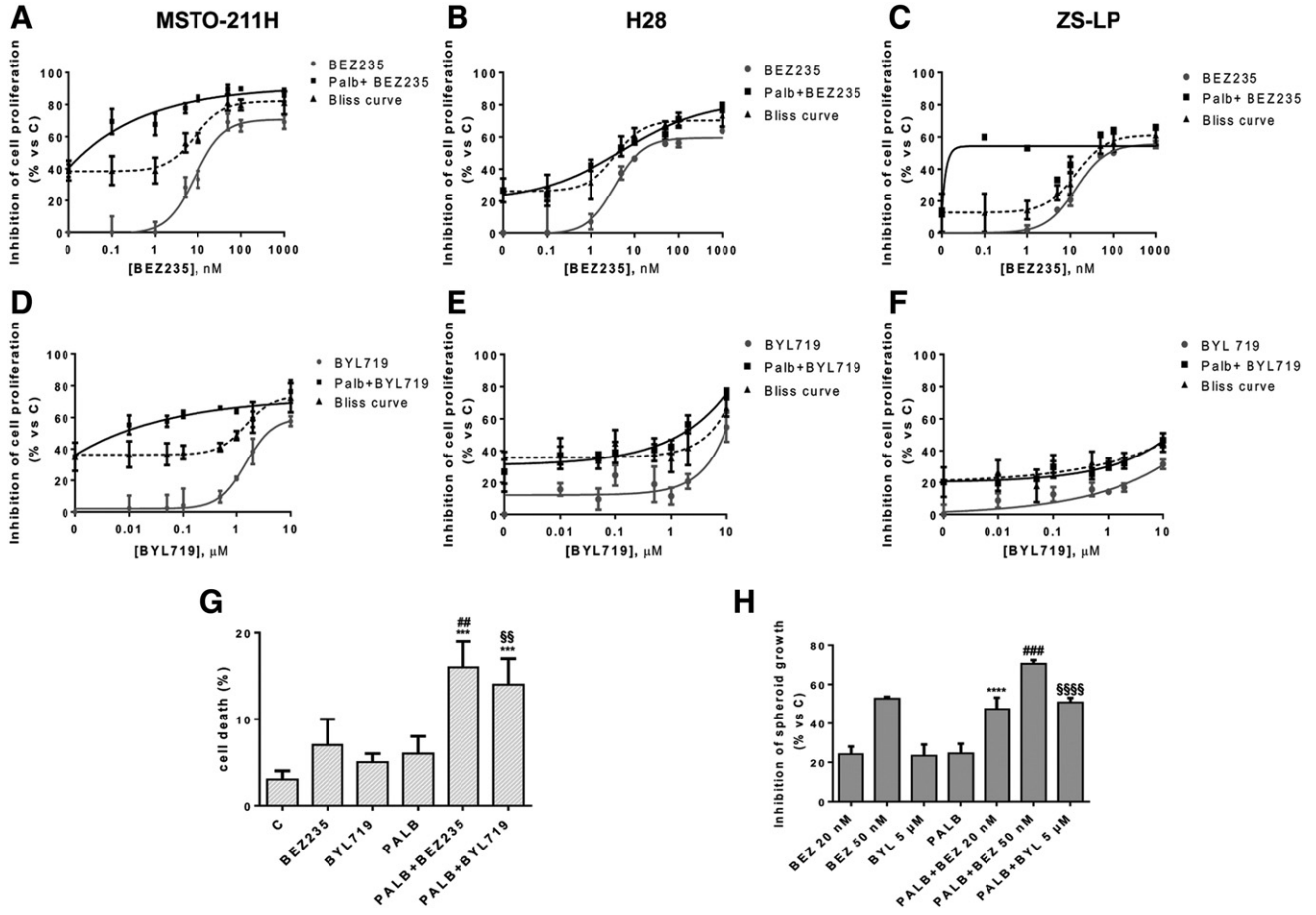

Figure 3. Effect of the sequential treatment of palbociclib and PI3K/mTOR inhibitors on cell growth. MSTO-211H, H28, ZS-LP cells were treated with palbociclib 0.5 μM for 24 h. Then the cells were treated with increasing concentration of BEZ235 (from 0.1 nM to 1 μM) (A-C) or BYL719 (from 0.01 to 10 μM) (D-F) alone or in association with 0.5 μM of palbociclib for further 48 h. Cells proliferation was assessed by MTT assay. The type of interaction (antagonistic, additive or synergistic) was evaluated through Bliss analysis. Data are expressed as a percentage of inhibition versus control. (G) MSTO-211H cells were treated with 0.5 μM palbociclib for 72 h, or with 50 nM BEZ235, 5 μM BYL719 for 48 h, or with palbociclib for 24 h and then with the drug combination for further 48 h. The cells were counted and the percentage of cell death was evaluated after Hoechst 33342 and Propidium Iodide staining. Data are expressed as a percentage of dead cells (***$P < .001$ versus C; $^{\#\#}P < .01$ versus BEZ235; $^{\S\S}P < .01$ versus BYL719; one-way analysis of variance followed by Bonferroni's post-test). (H) After 3 days of culture in low adhesion condition spheroids were treated with 20 or 50 nM BEZ235, 5 μM BYL719 as single treatment for 48 h, or with 0.5 μM palbociclib alone for 96 h, or with palbociclib for 48 h and then with the sequential combined treatment for further 48 h. The volume of spheroids was calculated and expressed as a percentage of inhibition versus control. All the experiments are the mean value ±SD of three independent measurements (****$P < .0001$ versus BEZ235 20 nM; $^{\#\#\#}P < .001$ versus BEZ235 50 nM; $^{\S\S\S\S}P < .0001$ versus BYL719; one-way analysis of variance followed by Bonferroni's post-test).

DNA was quantified by Qubit, Thermo Fisher Scientific (Waltham, MA). The TruSight Cancer kit (Illumina Inc., San Diego, CA) was used to analyze cell lines for 94 genes and 284 single nucleotide polymorphisms (SNPs) associated with a predisposition towards various cancers. This panel covers a total of 255 kb and includes the entire coding regions of the genes and exon-intron boundaries (±20 bp). The library was performed using 50 ng of DNA from the cell line and sequenced on the Illumina MiSeq platform using 2 x 151 bp in pair-end mode and run on an Illumina V2 sequencing flow cell according to manufactures' instruction.

Data Analysis and Variant Calling

Raw de-multiplexed reads from the MiSeq sequencer were aligned to the reference human genome (UCSC-Build37/hg19) using the Burrows–Wheeler algorithm [17], running in paired-end mode. To ensure good call quality and to reduce the number of false positives, samples underwent Base Quality Score Recalibration (BQSR), using the Genome Analysis Toolkit GATK, version 3.2.2 [18]. After BQSR, sequences around regions with insertions and deletions (indels) were realigned locally with GATK. MarkDuplicates (http://broadinstitute.github.io/picard) was used to remove duplicate read-pairs arisen as artifacts during either polymerase chain reaction amplification or sequencing. Regions with coverage of less than or equal to 200× were discarded for downstream analyses. Somatic variant analyses were used to detect mutations: single nucleotide variants (SNVs) were identified using MuTect version 1.1.7 [19] with standard parameters, and GATK IndelGenotyperV2 (with minFraction = 0.01 and minCnt = 5) was used to detect indels. Genomic and functional annotation of detected variants was made by Annovar [20]. Coverage statistics were performed by Depth of Coverage utility of GATK. BASH and R custom scripts were used to obtain the list of

low coverage (200×) regions per sample. We found 660 variants in MG-LP cells and 580 variants in ZS-LP cells. To identify the candidate variants we adopted a series of filters: exon and splicing variants, coverage variant >200× and a variant frequency of >10%, annotation into public databases (dbSNP, Clinical Variants, COSMIC).

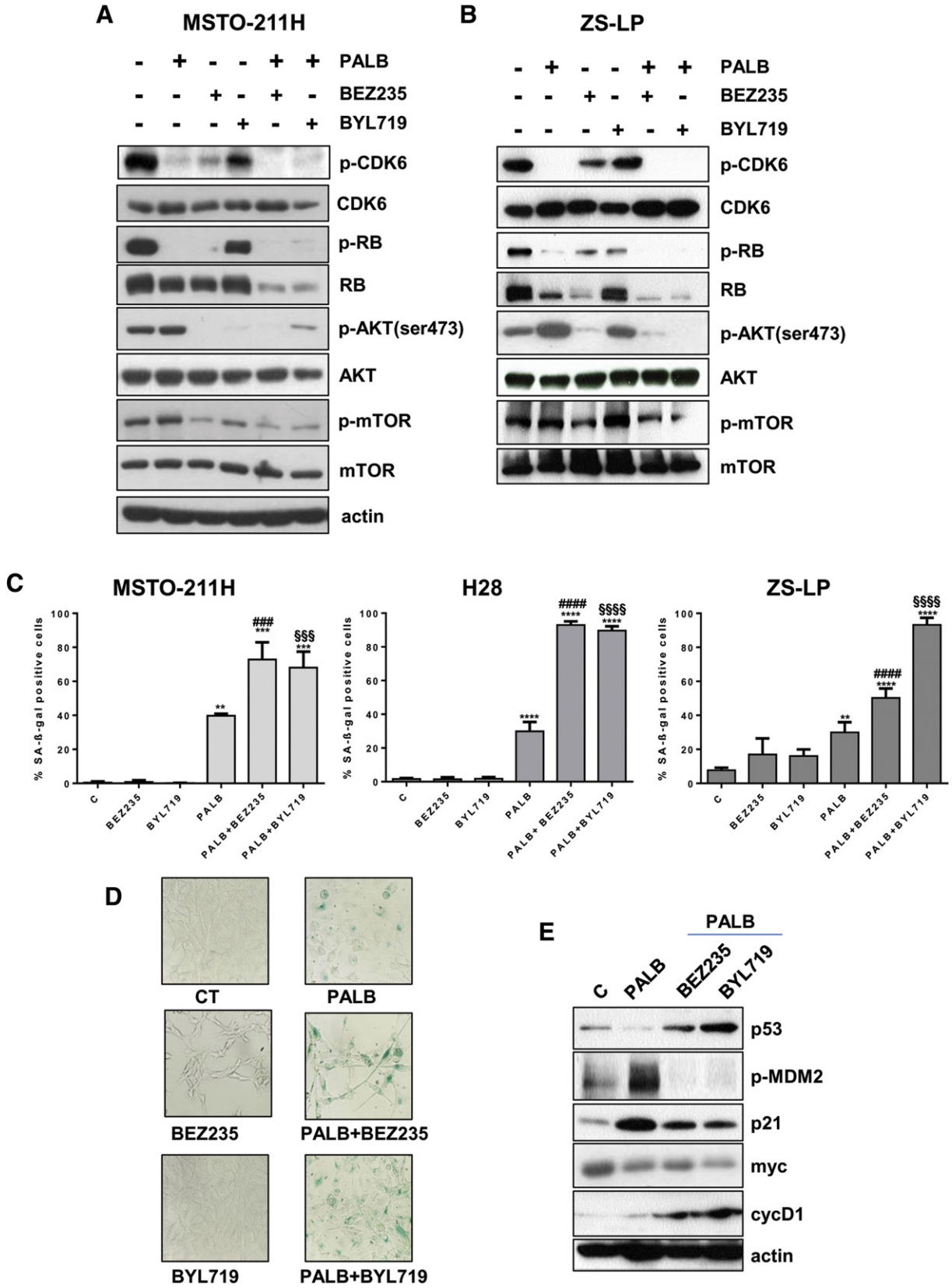

Statistical Analysis

Statistical analyses were carried out using GraphPad Prism 6.00 software (San Diego, CA). Statistical significance of differences among data was estimated by two-tailed Student's t test. Comparison among groups was made using analysis of variance (one-way ANOVA), followed by Bonferroni's post-test. Adjusted p values less than 0.05 were considered significant.

Results

Effects of Palbociclib Treatment in MPM Cell Lines

Low expression of $p16^{INK4a}$ and high levels of p-Rb and cyclin D1 have been identified as predictive factors of response to palbociclib in cancer cells [21]. We therefore performed Western blot and RT-PCR analyses to assess the baseline expression level of such proteins on a panel of MPM cell lines of different histotype and on two primary cell cultures (ZS-LP and MG-LP, biphasic histotype) obtained from pleural effusion of two MPM patients. All the cell models analyzed expressed detectable Rb, cyclin D1 and CDK6 protein levels (Figure 1*A*), and were negative for $p16^{INK4a}$ expression, as evaluated by RT-PCR (not shown).

Further characterization of ZS-LP and MG-LP primary cell cultures was performed by NGS analysis (table 1 and Supplementary Figure 1), confirming wild type gene expression for Rb and CDK4. In addition, we found *BAP1* gene deletion in MG-LP cells, *PMS2* gene (involved in DNA repair mechanism) deletion in ZS-LP cells, and *XPC* (involved in repair damaged DNA) and *CHRNA3* (associated with an increased risk to develop lung cancer) variants in both primary cell lines.

According to the expression of predictive markers of response to palbociclib, all the cell models were sensitive to the drug, with EC_{50} values ranging from 0.1 to 1.2 μM (Figure 1, *B* and *C*). By contrast, MDA-MB-468 breast cancer cells, characterized by the loss of Rb and intrinsically resistant to palbociclib [21], showed an EC_{50} value of 5 μM (Figure 1*C*).

As shown in Figure 2*A*, palbociclib induced a significant blockade of the progression from G1 to S phase of the cell cycle in all MPM sensitive cells; by contrast, the distribution among the cell cycle phases was unchanged in insensitive MDA-MB-468 cells. No signs of cell death were detected (not shown), thus confirming the cytostatic effect of the drug [21–23].

Interestingly, treatment with palbociclib induced an accumulation of senescent-like cells, characterized by the production of the Senescent-Associated β-galactosidase enzyme (SA-β-Gal) and by flat and enlarged cell morphology. As shown in Figure 2*B*, the percentage of senescent cells reached about 40% after 72 h of palbociclib treatment in MSTO-211H, and about 30% in H28 as well as in ZS-LP cells.

Then, we evaluated the expression level of different proteins involved in the regulation of the cell cycle and in signal transduction on MPM cell lines treated with palbociclib for 24 h. By inhibiting the cyclin D1/CDK4–6 complexes, palbociclib decreased the phosphorylation of CDK6 in all the cell lines analyzed; as a consequence Rb was hypo-phosphorylated, thus inhibiting the transcription factor E2F and the expression of myc, one of its target genes (Figure 2*C*). Interestingly palbociclib reduced also Rb total level. As previously reported for breast cancer cell lines [6], treatment with palbociclib up-regulated p-AKT and p-p70S6K levels in a dose-dependent manner also in MPM cells. In addition, the level of cyclin D1 was increased, confirming cyclin D1 induction as a marker associated to cellular senescence [24].

As demonstrated by a time-course experiment, all these molecular changes became evident after 24 h of palbocilib exposure, concomitantly with the inhibitory effect on cell cycle progression (Supplementary Figure 2). Moreover, the expression and phosphorylation of MAPK were not affected by palbociclib treatment.

Effects of Sequential Combined Treatment with Palbociclib and PI3K Inhibitors in MPM Cells

Considering the positive regulatory effect of palbociclib on AKT activation, we tested the efficacy of combining palbociclib with two inhibitors of the PI3K/AKT/mTOR pathway: BEZ235, a dual PI3K and mTORC1–2 inhibitor, and BYL719, an inhibitor of the p110α isoform of PI3K.

Since the induction of AKT phosphorylation reached the highest level after 24 h of treatment with palbociclib, we firstly treated the cells with a sequential drug treatment protocol: 24 h of palbociclib alone, followed by a combination of palbociclib with PI3K inhibitors for further 48 h. Using the Bliss additivism model, we observed a synergistic or additive inhibition of cell proliferation in MSTO-211H, H28, and ZS-LP cells (Figure 3, *A-F*). In addition, the sequential treatment induced a slight but significant increase (up to 16%) in the percentage of cell death (Figure 3*G*). We then tested the effect of a simultaneous treatment with palbociclib and PI3K inhibitors (Supplementary Figure 3). In H28 cells, in which the sequential treatment determined additivism, also the concomitant treatment induced an additive inhibition of cell proliferation. Differently, in MSTO-211H cells the synergistic inhibition observed with the sequential treatment was lost after the simultaneous drug treatment. On the basis of these results, the sequential drug combination was used for further experiments.

Figure 4. Effect of the sequential treatment of palbociclib and PI3K/mTOR inhibitors on signal transduction and senescence. (A-B) MSTO-211H and ZS-LP cells were treated with palbociclib 0.5 μM for 24 h. Then the cells were treated with 50 nM BEZ235 or 5 μM BYL719 alone or in association with palbociclib 0.5 μM for further 24 h. The cells were lysed and the expression of the indicated proteins was evaluated by Western blot analysis. The experiment repeated twice yielded similar results. (C) MSTO-211H, H28 and ZS-LP cells were treated with palbociclib 0.5 μM for 24 h. Then the cells were treated with BEZ235 (50 nM) or BYL719 (5 μM) alone or in association with palbociclib for 48 h. Histograms represent the percentage of senescent cells positive for SA-β-Gal expression (**$P < .01$, ***$P < .001$, ****$P < .0001$ versus C; $^{\#\#\#}P < .001$, $^{\#\#\#\#}P < .0001$ versus BEZ235; $^{§§§}P < .001$, $^{§§§§}P < .0001$ versus BYL719; one-way analysis of variance followed by Bonferroni's post-test). (D) Representative images of MSTO-211H cells treated as described in (C) and stained with SA-β-Gal Staining kit. (E) MSTO-211H cells were treated with palbociclib 0.5 μM for 24 h. Then the cells were treated with BEZ235 (50 nM) or BYL719 (5 μM) in association with palbociclib for further 48 h. The cells were lysed and the expression of the indicated proteins was assessed by Western blot analysis. The experiment repeated twice yielded similar results. Data in C are means ±SD of three independent experiments.

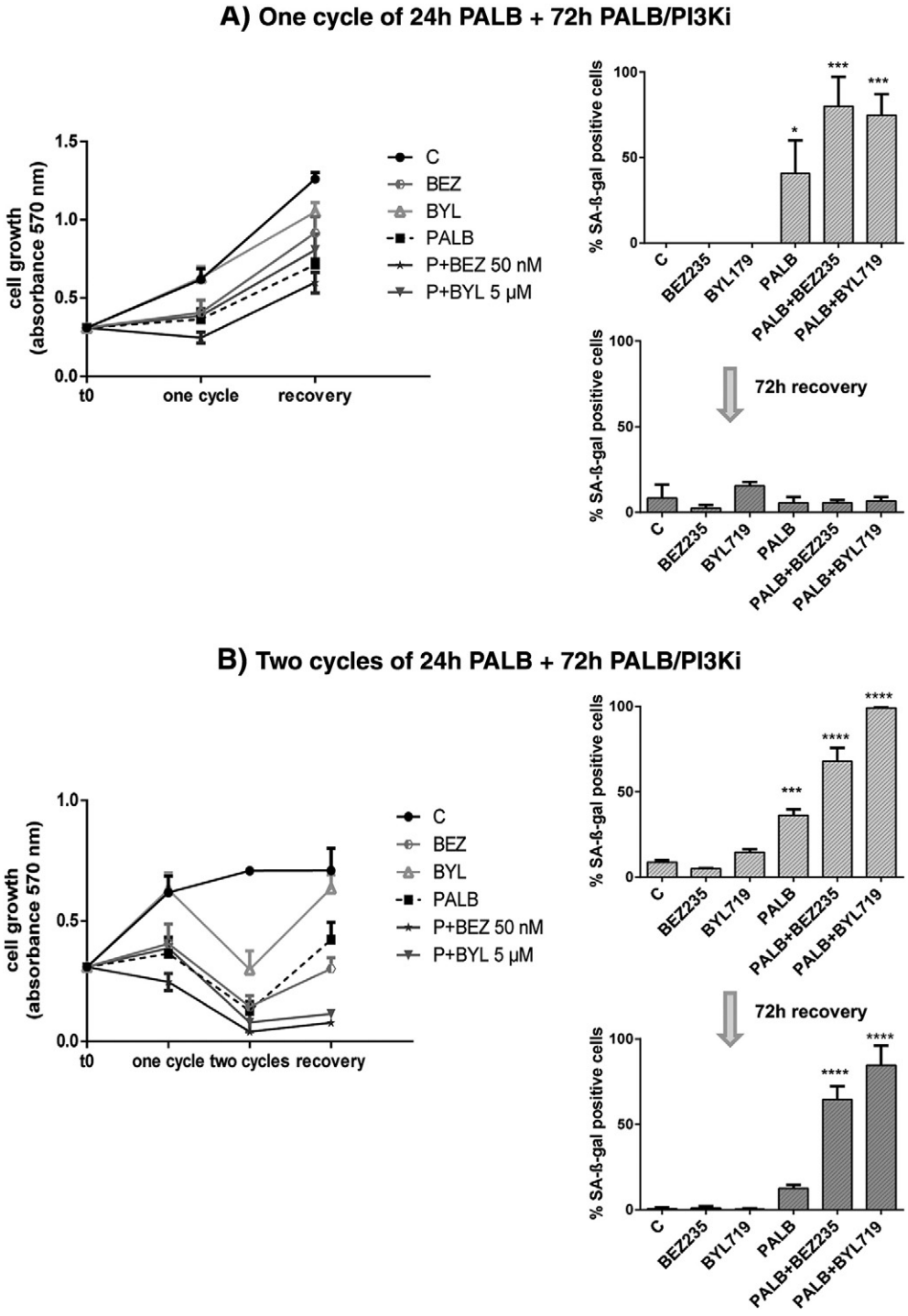

Figure 5. Effects of removal of palbociclib and PI3K inhibitors on cell proliferation and senescence induction. (A) MSTO-211H cells were treated for 24 h with palbociclib 0.5 μM and then with BEZ235 (50 nM) or BYL719 (5 μM) in association with palbociclib for 72 h, or with 0.5 μM palbociclib, 50 nM BEZ235 or 5 μM BYL719 alone for 96 h (one cycle); then cells were cultured for additional 72 h in the absence of the drugs (recovery time). After the treatment period and after the recovery time, cell proliferation was evaluated by crystal violet staining, and senescent cells were counted after staining for SA-β-Gal (*$P < .05$, ***$P < .001$ versus C; one-way analysis of variance followed by Bonferroni's post-test). (B) Cells were treated as described in A, but two cycles were performed. After these two cycles and after the recovery time, cell proliferation was evaluated by crystal violet staining and senescent cells were counted after staining for SA-β-Gal. Data in A and B are means ±SD of three independent experiments (***$P < .001$, ****$P < .0001$ versus C; one-way analysis of variance followed by Bonferroni's post-test).

The greater efficacy of the sequential combined treatment over individual activity was further confirmed in a three dimensional (3D) system using MSTO-211H cells (Figure 3*H*).

The additive/synergistic inhibitory effects of the drug combination on cell proliferation were associated with a significant down-regulation of p-CDK6, p-Rb, Rb levels, as well as with the inhibition

of the AKT/mTOR pathway in both MSTO and ZS-LP cells (Figure 4, *A* and *B*).

Subsequently, we evaluated the impact of the sequential drug treatment on either cell cycle-phase distribution and senescence in MSTO-211H, H28 and ZS-LP MPM cells. After sequential treatment, the cells were almost completely blocked in G0-G1 phase with values ranging from 90% to 95% depending on cell type. Moreover, the percentage of senescent cells was further increased after palbociclib/PI3Ki sequential treatment in comparison with palbociclib alone (60–90% versus 30–40%) in all the analyzed cell models (Figure 4, *C* and *D*).

Interestingly, as shown in Figure 4*E*, palbociclib treatment induced a significant phosphorylation of MDM2, probably as a consequence of AKT activation, thus hindering the accumulation of p53 protein. Under this condition, we observed a great increase in p21 expression, that might be ascribed to the release of *p21* gene negative regulation exerted by myc, or to AKT/mTOR signaling activation (as previously shown, Figure 2), which has been shown to initiate p21-dependent senescence in particular conditions [24].

In contrast, when palbociclib was combined with PI3K/mTOR inhibitors, MDM2 phosphorylation was down-regulated, allowing p53 accumulation and p21 induction. These results suggest that the induction of senescence by palbociclib alone or in combination may be ascribed to different mechanisms.

Effects of Removal of Palbociclib and PI3K Inhibitors on Cell Proliferation and Senescence Induction

To test for the reversibility of the sequential treatment with palbociclib and PI3K inhibitors, MSTO-211H cells were treated for one cycle with the drugs (24 h palbociclib followed by 72 h with the combination of palbociclib and PI3K inhibitors, or 96 h with the single drug); then the medium was replaced with drug-free medium and the cells were cultured for additional 72 h. After the recovery period, the cells completely re-acquired the proliferative capability, as shown by crystal-violet staining assay (Figure 5*A*), and the senescent phenotype was completely lost (Figure 5*A*) both after the sequential combined treatments as well as after single drug treatments. We then exposed MSTO-211H cells to two cycles of treatment, followed by 72 h of recovery in drug-free medium, and we evaluated both inhibition of cell proliferation and senescence induction. After such a prolonged treatment, cell growth was blocked irreversibly and the senescent phenotype was maintained both in MSTO-211H cells (Figure 5*B*) as well as in H28 cells (Supplementary Figure 4) only when the cells were exposed to the sequential combined treatment. Conversely, cells treated with palbociclib or PI3K inhibitors alone showed a recovery of cell proliferation and hence a reduction of the percentage of senescent cells after drug removal, indicating that the effects induced by palbociclib or PI3K inhibitors were reversible even after a prolonged treatment.

Discussion

Although several studies and clinical trials have been conducted over the last decade, cure opportunities for MPM have not significantly improved, and the new most promising targeted approaches (i.e. anti-angiogenic treatment, anti-immune-checkpoints inhibitors) are still under clinical evaluation [2]. Such unfavorable outcomes are due in part to the fact that the current chemotherapy does not leverage the characteristic biological features of this disease. In addition, most of the alterations involved in MPM oncogenesis are due to inactivation of tumor suppressor genes, rather than driver mutations in oncogenic

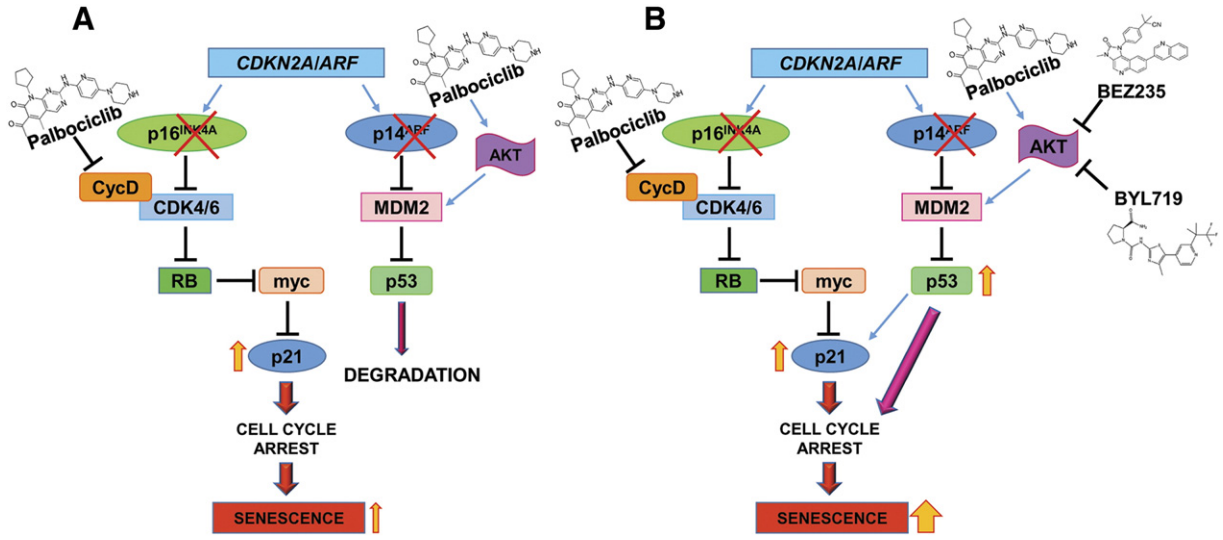

Figure 6. Representative scheme of the mechanisms involved in the induction of cell cycle arrest and senescence. MPM cell lines are frequently deleted in *CDKN2A/ARF* gene, coding for both $p16^{INK4a}$ and $p14^{ARF}$. (A) Palbociclib treatment, by inhibiting cyclin D1/CDK4/6 complexes, impeded Rb hyper-phosphorylation, preventing E2F release and the consequent induction of E2F induced genes, as *myc*. By binding to *p21* promoter, myc inhibited p21 gene transcription and expression. Under palbociclib treatment this mechanism was lost and p21 accumulated, inducing cell cycle arrest and senescence. On the other hand, the loss of the MDM2-inhibitor $p14^{ARF}$ hindered the accumulation of p53. Moreover, the inhibition of CDK4/6 determined by palbociclib treatment, by increasing p-AKT level, induced the accumulation of p-MDM2 that, as a consequence, promoted p53 degradation. (B) The sequential combined treatment with palbociclib and PI3K inhibitors, by blocking the PI3K pathway, inhibited AKT and strongly down-regulated p-MDM2, thus allowing p53 accumulation and the induction of cellular senescence.

genes [3,4], thus making the development of new therapies more difficult.

The most frequent altered gene in MPM patients is *CDKN2A/ARF* encoding for the cell cycle suppressors $p16^{INK4a}$ and $p14^{ARF}$. Our findings demonstrate that *CDKN2A/ARF* gene alterations represent an attractive target for MPM treatment. We investigated the effects of the CDK4/6 inhibitor palbociclib on a panel of four commercial cell lines of MPM of different histotype and on two primary cultures isolated from pleural effusion of MPM patients. All the cell lines analyzed showed the presence of the predictive markers of response to palbociclib, i.e. Rb, cyclin D1, and CDK6 expression, as well as the absence of $p16^{INK4a}$, and were sensitive to palbociclib treatment. By NGS analysis we identified additional mutations in primary cell cultures in genes involved in DNA repair (PMS2, XPC) and associated with the risk of lung cancer development (CHRNA3); however these alterations did not affected palbociclib sensitivity. As previously reported for other cancer cell models, palbociclib exerted a cytostatic effect, promoting an accumulation in the G0-G1 phase of the cell cycle.

It has been reported that inhibition of CDK4/6 can induce cellular quiescence or senescence, depending on the tumor cell type [25–28]. Exposure to palbociclib promoted senescence in MPM cells, with a nearly 30% SA-βgal positive cells after 3 days and 40% after 8 days of treatment. However, after palbociclib removal, the cells re-acquired the proliferative capability, indicating that the majority of them were in a quiescent state. This reversible cell cycle arrest has also been documented in hepatocellular carcinoma cells exposed to a prolonged treatment with palbociclib and then recovered in drug-free medium [22]. The mechanisms underlying the induction of quiescence or senescence by CDK4/6 inhibitors are not completely defined, although p53-independent mechanisms seem to be involved. For example, treatment with the CDK4/6 inhibitor LE001 in neuroblastoma cell lines has been shown to promote senescence through down-regulation of the FOXM1 transcription factor [23]. In addition, it has been demonstrated in liposarcoma cells that the loss of MDM2 together with the expression of ATRX are involved in the induction of a senescent phenotype; interestingly, MDM2 was shown to regulate senescence in a p53-independent manner, through direct ubiquitination of a senescence-activating protein (SAP) [25].

Our results demonstrate that in MPM cell models palbociclib promoted cell cycle arrest and senescence associated with a p53-independent induction of p21 protein. *p21* gene expression is negatively regulated by the transcriptional factor myc, that binds directly to *p21* promoter inhibiting gene transcription [29,30]. Under palbociclib treatment, Rb was hypo-phosphorylated and myc level decreased as a consequence of Rb-mediated inhibition of E2F, thus allowing p21 accumulation. The role of myc suppression in the induction of cellular senescence has been already described in melanoma cell lines. In particular, myc depletion has been demonstrated to favor the emergence of a senescent phenotype associated with oncogene over-expression independently of p53 [31]. In addition to this mechanism, we cannot rule out the involvement of active mTOR in palbociclib-mediated induction of senescence. Indeed, we demonstrated that palbocilcib activates AKT and its downstream target mTOR, which in turn has been shown to initiate senescence in the presence of p21 and elevated cyclin D1 [24]. P53 was not involved in these processes, since palbociclib treatment, by increasing p-AKT levels, induced the accumulation of p-MDM2, that, in turn promoted p53 degradation.

Palbociclib-induced phosphorylation of AKT has also been observed in osteosarcoma and breast cancer cells [6] and has been ascribed to the release of the negative regulation towards mTORC2 kinase complex mediated by hyper-phosphorylated Rb. Indeed, in addition to the canonical inhibitory function of hypo-phosphorylated Rb towards E2F, the authors described a new mechanism of action of Rb. In the cytoplasm, hyper-phosphorylated Rb directly binds Sin1, a component of mTORC2 complex, thus inhibiting the complex activity. Since AKT is a substrate of mTORC2, the inhibition of Rb phosphorylation, due to CDK4/6 inhibition, promoted mTORC2 activation and as a consequence increased AKT activation [6].

The increased phosphorylation/activation of AKT mediated by palbociclib provided a rationale for combining this drug with PI3K/mTOR inhibitors following a sequential combined protocol. We demonstrated that the combined sequential treatment induced a synergistic/additive inhibition of cell proliferation in MPM cells, both in 2D and 3D culture, while the simultaneous treatment with palbociclib and PI3K inhibitors gave rise only to an additive effect according to Bliss experimental model. Indeed, treatments with CDK4/6 inhibitors alone significantly promoted AKT activation, and the following sequential treatment with CDK4/6 and PI3K/mTOR inhibitors reduced the phosphorylation of both Rb and AKT-ser473; as a consequence, mTOR activation was impaired. As recently reported, co-treatment with CDK4/6 and AKT inhibitors demonstrated a synergistic reduction of cell viability and increased cell apoptosis in Rb-proficient, but not Rb-deficient breast cancer cells [6]. Apoptosis induction was also observed in mantle cell lymphoma after treatment with ON123300, a dual inhibitor of CDK4 and PI3K-δ and was ascribed to the inhibition of FOXO1 activation [32]. In contrast, in MPM cell lines we observed only a slight increase in apoptotic death after the sequential combined treatment with palbociclib and PI3K/mTOR inhibitors, whereas a significant percentage of cells (ranging from 60 to 85% depending on the cell line) underwent senescence.

In contrast to palbociclib treatment, the sequential drug treatment induced cellular senescence through p53. In particular, the blockade of PI3K pathway, by inhibiting AKT, strongly down-regulated p-MDM2, thus allowing p53 accumulation and the induction of cellular senescence.

Our results suggest that the induction of cellular senescence is regulated by p53-independent or -dependent mechanisms when palbociclib is given alone or in combination with PI3K inhibitors, respectively (Figure 6).

Our findings also demonstrated that even a prolonged treatment (8 days) with palbociclib alone failed to maintain the inhibition of cell proliferation when palbociclib was removed. In particular, palbociclib alone induced cell cycle arrest in almost all the cells, whereas the induction of senescence never exceeds 50% of the total cell population. This finding suggests that most of the quiescent cells re-acquired the proliferative capability after drug removal, enlightening the reversible action of the drug. The same behavior has been recently observed in hepatocellular carcinoma cells after a prolonged treatment with palbociclib [22]. Also the prolonged treatment with PI3K inhibitors was reversible and, after drug removal, the cells reacquired the proliferative capability. Moreover we failed to detect senescent cells with PI3K inhibitors alone, even after two cycles of treatment. By contrast, we show that when palbociclib treatment was followed by the combination with PI3K inhibitors, the percentage of

senescent cells was increased, although at least two schedules were required to induce an irreversible cell cycle arrest, hindering cell proliferation even after drug removal.

Conclusions

Considering that loss of *CDKN2A/ARF* is a common alteration in MPM, our study is the first demonstrating the effectiveness of palbociclib in this tumor. Moreover, the association of palbociclib with PI3K inhibitors showed a synergistic/additive interaction on the inhibition of cell growth and had an irreversible effect on the inhibition of cell proliferation and the induction of senescence. Collectively our results demonstrate that the association of palbociclib with PI3K inhibitors may represent a valuable new therapeutic approach for MPM treatment.

Supplementary data to this article can be found online at http://dx.doi.org/10.1016/j.neo.2017.05.003.

Ethics Approval and Consent to Participate

The procedure was approved by the institutional review board for human studies (Ethical Committee) of the University-Hospital of Parma and in accord with principles listed in the Helsinki declaration. Patients were enrolled after informed consent to the employment of biologic samples for research purpose.

Competing Interests

The authors declare that they have no competing interests.

Acknowledgements

Not applicable.

References

[1] Craighead JE (2011). Epidemiology of mesothelioma and historical background. *Recent Results Cancer Res* **189**, 13–25.
[2] Bonelli MA, Fumarola C, La Monica S, and Alfieri R (2017). New therapeutic strategies for malignant pleural mesothelioma. *Biochem Pharmacol* **123**, 8–18.
[3] Sekido Y (2013). Molecular pathogenesis of malignant mesothelioma. *Carcinogenesis* **34**, 1413–1419.
[4] Hylebos M, Van Camp G, van Meerbeeck JP, and Op de Beeck K (2016). The Genetic Landscape of Malignant Pleural Mesothelioma: Results from Massively Parallel Sequencing. *J Thorac Oncol* **11**, 1615–1626.
[5] Ruas M and Peters G (1998). The p16INK4a/CDKN2A tumor suppressor and its relatives. *Biochim Biophys Acta* **1378**, F115–F177.
[6] Zhang J, Xu K, Liu P, Geng Y, Wang B, Gan W, Guo J, Wu F, Chin YR, and Berrios C, et al (2016). Inhibition of Rb Phosphorylation Leads to mTORC2-Mediated Activation of Akt. *Mol Cell* **62**, 929–942.
[7] Efeyan A and Sabatini DM (2010). mTOR and cancer: many loops in one pathway. *Curr Opin Cell Biol* **22**, 169–176.
[8] Maira SM, Stauffer F, Brueggen J, Furet P, Schnell C, Fritsch C, Brachmann S, Chene P, De Pover A, and Schoemaker K, et al (2008). Identification and characterization of NVP-BEZ235, a new orally available dual phosphatidylinositol 3-kinase/mammalian target of rapamycin inhibitor with potent in vivo antitumor activity. *Mol Cancer Ther* **7**, 1851–1863.
[9] Furet P, Guagnano V, Fairhurst RA, Imbach-Weese P, Bruce I, Knapp M, Fritsch C, Blasco F, Blanz J, and Aichholz R, et al (2013). Discovery of NVP-BYL719 a potent and selective phosphatidylinositol-3 kinase alpha inhibitor selected for clinical evaluation. *Bioorg Med Chem Lett* **23**, 3741–3748.
[10] Cavazzoni A, Alfieri RR, Carmi C, Zuliani V, Galetti M, Fumarola C, Frazzi R, Bonelli M, Bordi F, and Lodola A, et al (2008). Dual mechanisms of action of the 5-benzylidene-hydantoin UPR1024 on lung cancer cell lines. *Mol Cancer Ther* **7**, 361–370.
[11] Alfieri RR, Galetti M, Tramonti S, Andreoli R, Mozzoni P, Cavazzoni A, Bonelli M, Fumarola C, La Monica S, and Galvani E, et al (2011). Metabolism of the EGFR tyrosin kinase inhibitor gefitinib by cytochrome P450 1A1 enzyme in EGFR-wild type non small cell lung cancer cell lines. *Mol Cancer* **10**, 143.
[12] Cavazzoni A, Bonelli MA, Fumarola C, La Monica S, Airoud K, Bertoni R, Alfieri RR, Galetti M, Tramonti S, and Galvani E, et al (2012). Overcoming acquired resistance to letrozole by targeting the PI3K/AKT/mTOR pathway in breast cancer cell clones. *Cancer Lett* **323**, 77–87.
[13] Goldoni M and Johansson C (2007). A mathematical approach to study combined effects of toxicants in vitro: evaluation of the Bliss independence criterion and the Loewe additivity model. *Toxicol In Vitro* **21**, 759–769.
[14] Fumarola C, La Monica S, Alfieri RR, Borra E, and Guidotti GG (2005). Cell size reduction induced by inhibition of the mTOR/S6K-signaling pathway protects Jurkat cells from apoptosis. *Cell Death Differ* **12**, 1344–1357.
[15] La Monica S, Madeddu D, Tiseo M, Vivo V, Galetti M, Cretella D, Bonelli M, Fumarola C, Cavazzoni A, and Falco A, et al (2016). Combination of Gefitinib and Pemetrexed Prevents the Acquisition of TKI Resistance in NSCLC Cell Lines Carrying EGFR-Activating Mutation. *J Thorac Oncol* **11**, 1051–1063.
[16] Bonelli MA, Cavazzoni A, Saccani F, Alfieri RR, Quaini F, La Monica S, Galetti M, Cretella D, Caffarra C, and Madeddu D, et al (2015). Inhibition of PI3K Pathway Reduces Invasiveness and Epithelial-to-Mesenchymal Transition in Squamous Lung Cancer Cell Lines Harboring PIK3CA Gene Alterations. *Mol Cancer Ther* **14**, 1916–1927.
[17] Li H and Durbin R (2009). Fast and accurate short read alignment with Burrows-Wheeler transform. *Bioinformatics* **25**, 1754–1760.
[18] McKenna A, Hanna M, Banks E, Sivachenko A, Cibulskis K, Kernytsky A, Garimella K, Altshuler D, Gabriel S, and Daly M, et al (2010). The Genome Analysis Toolkit: a MapReduce framework for analyzing next-generation DNA sequencing data. *Genome Res* **20**, 1297–1303.
[19] Cibulskis K, Lawrence MS, Carter SL, Sivachenko A, Jaffe D, Sougnez C, Gabriel S, Meyerson M, Lander ES, and Getz G (2013). Sensitive detection of somatic point mutations in impure and heterogeneous cancer samples. *Nat Biotechnol* **31**, 213–219.
[20] Wang K, Li M, and Hakonarson H (2010). ANNOVAR: functional annotation of genetic variants from high-throughput sequencing data. *Nucleic Acids Res* **38**e164.
[21] Finn RS, Dering J, Conklin D, Kalous O, Cohen DJ, Desai AJ, Ginther C, Atefi M, Chen I, and Fowst C, et al (2009). PD 0332991, a selective cyclin D kinase 4/6 inhibitor, preferentially inhibits proliferation of luminal estrogen receptor-positive human breast cancer cell lines in vitro. *Breast Cancer Res* **11**, R77.
[22] Bollard J, Miguela V, Ruiz de Galarreta M, Venkatesh A, Bian CB, Roberto MP, Tovar V, Sia D, Molina-Sanchez P, and Nguyen CB, et al (2016). Palbociclib (PD-0332991), a selective CDK4/6 inhibitor, restricts tumour growth in preclinical models of hepatocellular carcinoma. *Gut*. http://dx.doi.org/10.1136/gutjnl-2016-312268.
[23] Rader J, Russell MR, Hart LS, Nakazawa MS, Belcastro LT, Martinez D, Li Y, Carpenter EL, Attiyeh EF, and Diskin SJ, et al (2013). *Dual CDK4/CDK6 inhibition induces cell-cycle arrest and senescence in neuroblastoma*. *Clin Cancer Res* **19**, 6173–6182.
[24] Leontieva OV and Blagosklonny MV (2013). *CDK4/6-inhibiting drug substitutes for p21 and p16 in senescence: duration of cell cycle arrest and MTOR activity determine geroconversion*. *Cell Cycle* **12**, 3063–3069.
[25] Kovatcheva M, Liu DD, Dickson MA, Klein ME, O'Connor R, Wilder FO, Socci ND, Tap WD, Schwartz GK, and Singer S, et al (2015). *MDM2 turnover and expression of ATRX determine the choice between quiescence and senescence in response to CDK4 inhibition*. *Oncotarget* **6**, 8226–8243.
[26] Wiedemeyer WR, Dunn IF, Quayle SN, Zhang J, Chheda MG, Dunn GP, Zhuang L, Rosenbluh J, Chen S, and Xiao Y, et al (2010). *Pattern of retinoblastoma pathway inactivation dictates response to CDK4/6 inhibition in GBM*. *Proc Natl Acad Sci U S A* **107**, 11501–11506.
[27] Zou X, Ray D, Aziyu A, Christov K, Boiko AD, Gudkov AV, and Kiyokawa H (2002). *Cdk4 disruption renders primary mouse cells resistant to oncogenic transformation, leading to Arf/p53-independent senescence*. *Genes Dev* **16**, 2923–2934.
[28] Baughn LB, Di Liberto M, Wu K, Toogood PL, Louie T, Gottschalk R, Niesvizky R, Cho H, Ely S, and Moore MA, et al (2006). *A novel orally active small molecule potently induces G1 arrest in primary myeloma cells and prevents tumor growth by specific inhibition of cyclin-dependent kinase 4/6*. *Cancer Res* **66**, 7661–7667.
[29] Karimian A, Ahmadi Y, and Yousefi B (2016). *Multiple functions of p21 in cell cycle, apoptosis and transcriptional regulation after DNA damage*. *DNA Repair (Amst)* **42**, 63–71.

[30] Wu S, Cetinkaya C, Munoz-Alonso MJ, von der Lehr N, Bahram F, Beuger V, Eilers M, Leon J, and Larsson LG (2003). *Myc represses differentiation-induced p21CIP1 expression via Miz-1-dependent interaction with the p21 core promoter*. *Oncogene* **22**, 351–360.

[31] Zhuang D, Mannava S, Grachtchouk V, Tang WH, Patil S, Wawrzyniak JA, Berman AE, Giordano TJ, Prochownik EV, and Soengas MS, et al (2008). *C-MYC overexpression is required for continuous suppression of oncogene-induced senescence in melanoma cells*. *Oncogene* **27**, 6623–6634.

[32] Divakar SK, Ramana Reddy MV, Cosenza SC, Baker SJ, Perumal D, Antonelli AC, Brody J, Akula B, Parekh S, and Reddy EP (2016). *Dual inhibition of CDK4/Rb and PI3K/AKT/mTOR pathways by ON123300 induces synthetic lethality in mantle cell lymphomas*. *Leukemia* **30**, 86–93.